Dual Temperature- and pH-Dependent Self-Assembly of Cellulose-Based Copolymer with a Pair of Complementary Grafts

Shun Wan,[†] Ming Jiang,*[,†] and Guangzhao Zhang[‡]

The Key Laboratory of Molecular Engineering of Polymers of Ministry of Education, Department of Macromolecular Science, Fudan University, Shanghai 200433, China, and Hefei National laboratory for Physical Sciences at Microscale, Department of Chemical Physics, University of Science and Technology of China, Hefei, Anhui, China

Received January 18, 2007; Revised Manuscript Received May 8, 2007

ABSTRACT: Thermo- and pH-responsive micellization of HEC-*g*-(PNiPAAm&PAA) (CNiPAa) was studied. This binary graft copolymer CNipAa was synthesized via successive radical polymerization of *N*-isopropylacrylamide (NiPAAm) and acrylic acid (AA) from hydroxyethyl cellulose (HEC) as the backbone. The copolymers are able to self-assembly into a trinity of micelles of different structures by combined pH and temperature stimuli: (1) at 30 °C and a low pH range (<4.6), forming the micelles with a core of PAA/PNiPAAm due to hydrogen-bonding interaction between the two grafts; (2) in basic solution and at a temperature above the LCST of PNipAAm, hydrophobic aggregation of PNiPAAm grafts leading to PNiPAAm-core micelles with a compound shell of PAA/HEC; (3) forming a three-layer micellar structure due to the further response of the PNipAAm-core micelles to pH change. These three forms of micelles were examined by TEM, AFM, and DLS/SLS, and the corresponding forming mechanisms were clarified. As far as we know, it is the first report on so diverse micellization behavior of graft copolymers.

Introduction

Multiple stimuli-responsive (co)polymers soluble in water have attracted growing attention due to their diverse self-assembly behavior in response to multiple stimuli, such as pH, temperature, salt, etc.[1−19] Based on the manifold sensitivities, polymeric micelles with different structures can be obtained simply by changing environmental conditions; thus, it becomes possible to tailor micelles with desirable morphologies and properties for different potential applications from the same precursory copolymers. Up to now, dozens of such smart polymeric systems have been reported with dual sensitivities, unexceptionally from block copolymers.

The first report in this field is dealt with poly[2-(diethylamino)ethyl methacrylate-*b*-2-(*N*-morpholino)ethyl methacrylate] [PDEA-*b*-PMEMA][1,2] by Armes in 1998. The block copolymer was dissolved molecularly in water at pH 4 and formed PDEA-core micelles at pH 7−8 and PMEMA-core micelles when salt was added. The second example is poly[propylene oxide-*b*-2-(diethylamino)ethyl methacrylate] [PPO-*b*-PDEA],[3] in which PPO and PDEA are sensitive to temperature and pH, respectively. This copolymer existed as unimers at pH 6 and 5 °C and self-assembled into PDEA-core micelles at pH 8 and 5 °C as well as PPO-core micelles at pH 6 and 40 °C. Later on, various dual sensitive copolymers were reported, such as poly(4-vinylbenzoic acid) (PVBA)-containing block copolymers of [PVBA-*b*-PDEA][4] and [PVBA-*b*-PMEMA],[5] poly(methacrylic acid) (PDMA)-containing copolymers of [PDMA-*b*-PMAA][6] and [PDEA-*b*-PMAA],[7] and poly(succinyl ethyl methacrylate-*b*-DEA) [PSEMA-*b*-PDEA].[8] Obviously, for these systems, the majority of the blocks are not biodegradable, and no interactions, such as hydrogen bonding and electrostatic force, exist between the unlike blocks. Recently, Müller et al.[9,10] reported micellization of diblock copolymer composed of PAA and PNipAAm, which are pH and temperature sensitive, respectively. However, the copolymers would precipitate in water upon concurrent pH and temperature stimuli because PAA and PNipAAm being a complementary pair form an insoluble complex. In fact, almost all the AB diblock copolymers mentioned above show similar properties, namely, the micelles formed due to one stimulus would become unstable and precipitate when they undergo the other stimulus.

The stability of micelles to the combined stimuli can be achieved if one uses the triblock copolymer ABC. For example, owing to the hydrophilicity of block PEG, the block copolymer (PEG-*b*-P4VP-*b*-PNiPAAm)[11] is capable of giving three forms of micelles at different conditions due to the thermosensitivity of PNipAAm and pH sensitivity of P4VP. The resultant micelles maintain stability when the combined stimuli of pH and temperature are utilized. In addition, ABC triblock copolymer containing a cross-linkable middle block was found to be able to fabricate two forms of "SCK" (shell cross-linked knedel like) micelles at high concentration.[12] In addition, if there are interblock interactions, such as hydrogen bonding and electrostatic force, the triblock copolymer may self-assembly in solution into complex micellar structures. For example, PEO−PDEA−PSEMA has interblock hydrogen bonds or electrostatic interactions when environmental condition changes. As a result, "trinity" micelles can be observed simply by adjusting the pH and temperature of the solutions.[13]

Our group reported that graft copolymer HEC-*graft*-PAA self-assembles into pH-induced micelles in water, and after cross-linking PAA, the resultant micelles undergo a pH-dependent transition between micelles and hollow spheres.[14] It was found that the pH-dependent hydrogen bonding between PAA and HEC is responsible for the micellization and the morphology transition. In this paper, we study a new binary graft copolymer, HEC-*graft*-PNipAAm&PAA (CNipAa), which is composed of biodegradable material (HEC) as the backbone and a pair of complementary sensitive polymers, PAA and PNipAAm, as the

* To whom the correspondence should be addressed. E-mail: mjiang@fudan.edu.cn.
[†] Fudan University.
[‡] University of Science and Technology of China.

10.1021/ma070147b CCC: $37.00
Published on Web 06/20/2007

Table 1. Characteristic Data of HEC, CNip, and CNipAa Graft Copolymers

samples	NiPAAm/AGU/AA (mol %)[a]	$M_w \times 10^{-4}$ [b]	av graft points of PNipAAm/PAA per HEC backbone	length of PNipAAm/PAA grafts, $M\eta \times 10^{-4}$ [c]	$\langle D_h \rangle$/ nm[d]
HEC	0/100/0	11.9	0/0		40.4
CNip	74.6/25.4/0	24.6	15.6/0	0.81/0	56.4
CNipAa	54.4/18.4/27.2	33.8	15.6/5.6	0.81/1.63	68.0

[a] The molar ratio of *N*-isopropylacrylamide and acrylic acid units to AGU (anhydroglucose) was determined by elementary analysis (EA). [b] Obtained by SLS in neutral water (Figure S10); d*n*/d*c* for HEC, CNip, and CNipAa is 0.135, 0.161, and 0.141, respectively. [c] Calculated from viscosity measurements. [d]Measured by DLS at the same condition as for SLS.

two grafts. This graft copolymer can molecularly dissolve in water and self-assemble into three forms of micelles by tuning pH and temperature based on the thermosensitivity of PNipAAm, the pH sensitivity of PAA, and the interpolymer hydrogen bonding in low pH region. More interestingly, the micelles are very stable to the combined changes of pH and temperature over a wide range, which is rarely reported in the literature. As far as we know, it is the first dual pH- and temperature-sensitive system based on non-block copolymers, which have many advantages in synthesis: surfactant-free, nontoxicity, and organic reagent-free. It is worthy noting that the materials used here including HEC, PNiPAAm, and PAA are environmental-friendly polymers and have already been used in biorelated researches for many years; thus, the resultant micelles have great potential in applications.

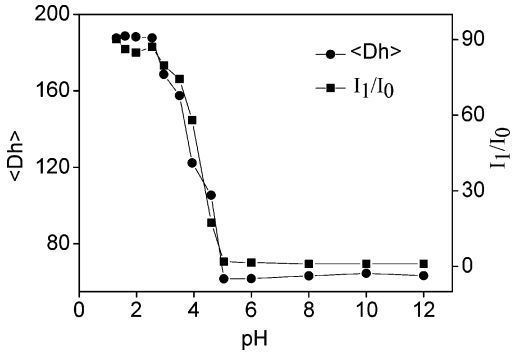

Figure 1. $\langle D_h \rangle$ and I_1/I_0 of CNipAa copolymers as a function of pH at 30 °C. The concentration was 1 mg/mL. I_1 and I_0 are the scattering intensity at the given pH values and pH 12, respectively.

Experimental Section

Polymer Synthesis and Characterization. Binary graft copolymers HEC-*g*-PNipAAm-PAA (CNipAa) were synthesized through successive cerium(IV)-initiated free-radical copolymerization of *N*-isopropylacrylamide (NiPAAm) and acrylic acid (AA), from HEC backbone. HEC used with high solubility in water was a product of hydroethylation of commercial HEC (Supporting Information). The resultant copolymers CNip and CNipAa were fully characterized by ^{1}H NMR, FT-IR, and elementary analysis (EA). The hydrodynamic diameters and average molecular weights of HEC, CNip, and CNipAa were measured by dynamic and static light scattering (DLS and SLS), respectively (Table 1). In order to know the average graft length and graft density (the number of grafts per HEC backbone), the backbone of CNipAa copolymer was fully biodegraded with cellulase, and then the PNiPAAm and PAA grafts were recovered for viscosity measurements. From the composition, total molecular weight of the copolymers, and the molecular weights of the grafts, the graft densities are calculated. As either the copolymers or the grafts are of broad polydispersity, the calculated average graft densities are only an approximate estimation (Table 1). The details of the synthesis and characterization of the copolymers can be found in the Supporting Information.

Micellar Characterization. *Laser Light Scattering.*[20,21] Malvern Autosizer 4700 and ALV/SP-125 laser light scattering (LLS) spectrometers were used. LLS measurements were performed at a scattering angle range from 15° to 150°. DLS were performed at a scattering angle of 90°, except the cases for $\langle R_g \rangle / \langle R_h \rangle$ calculation where the measurement angle covers a range from 15° to 90°. The $\langle D_h \rangle$ and polydispersity index (PDI, $\mu 2/\Gamma^2$) were obtained by a cumulant analysis. Both DLS and SLS measurements for the micellar solutions were performed at a concentration of 1 mg/mL giving apparent values (Supporting Information).

Turbidity Measurement. The light transmittance of the micellar solutions was monitored as a function of pH or temperature at a fixed wavelength of 500 nm by means of a Perkin-Elmer Lamda 35 UV/vis spectrophotometer, equipped with a circulating water bath. The aqueous polymer concentration of 1.0 mg/mL was used. For the cases of temperature-varying process, the operation was conducted with a programmed temperature increasing from 25 to 55 °C and from 30 to 40 °C; the increasing rate was 1 °C/30 min.

Transmission Electron Microscopy (TEM). TEM observations were performed on a Philips CM 120 electron microscope at an accelerating voltage of 80 kV. A small drop from the micellar solutions kept at a given temperature was deposited onto preheated carbon-coated coppers EM grid and then dried at the same temperature.

Atom Force Microscopy (AFM). AFM observations were conducted with a Nanoscope microscope; the sample preparation was similar to that for TEM, but new cleaved mica was used as substrate.

Fluorescence probing steady-state fluorescence spectra were recorded on a Perkin-Elmer LS50B luminescence spectrometer equipped with a circulating water bath for controlling temperature. The aqueous polymer concentration of 1.0 mg/mL was used. All the measurements were conducted with either various pH values at 30 °C or a programmed temperature as that for the turbidity measurements. Pyrene, from acetone stock solution 1×10^{-5} M, was used as a micropolarity-sensitive probe in a final concentration 2×10^{-7} M. The excitation wavelength was 334 nm. The change in the intensity ratio (I_1/I_3) of the first (I_1) and the third (I_3) vibronic band, at 373 and 384 nm, respectively, in emission spectra was measured.

Results and Discussion

pH-Induced Micellization of CNipAa Copolymer. Graft copolymers CNipAa comprising natural material HEC as the backbone and a pair of complementary polymers, PNipAAm and PAA, as the grafts can dissolve molecularly in basic water and aggregate spontaneously upon appropriate pH changes. This course was monitored by DLS, and the results of the hydrodynamic diameter $\langle D_h \rangle$ and the ratio I_1/I_0 of the CNipAa copolymer solutions as a function of pH are shown in Figure 1. It is clear that both $\langle D_h \rangle$ and I_1/I_0 were low and remain invariant in a wide pH range of 12.0−5.0, indicating that CNipAa copolymers exist as unimers in water. However, when pH decreases to 4.6, both I_1/I_0 and $\langle D_h \rangle$ jump sharply. I_1/I_0 increases by about a factor of 80, and $\langle D_h \rangle$ rises to about 185 nm when pH decreased to 3. Obviously, CNiPAa copolymers experience a unimer−aggregate transition caused by pH changes. In addition, the transition was found to be reversible; namely, the aggregates can dissociate into unimers when the solution pH tuned back to above 5.

This aggregation behavior of CNipAa resembles that of HEC-*graft*-PAA reported previously.[14] For the latter case, we demonstrated that it is not the conformational changes of poly(acrylic acid) (PAA) but interpolymer complexation between

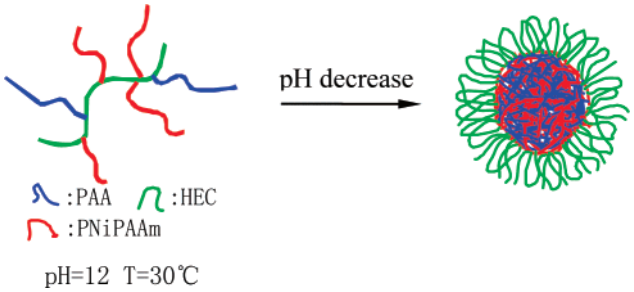

Figure 2. A proposed scheme of the formation of pH-induced micelles of CNipAa copolymers in water.

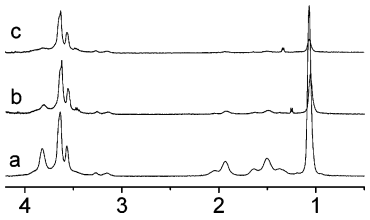

Figure 3. ^{1}H NMR spectra of CNipAa copolymer solution with differing pH values: (a) pH 12.3, (b) pH 4.3, and (c) pH 1.3.

PAA and HEC that is responsible for the micellization as pH decreases. Specifically, when pH decreases to about 3, most acrylic acid groups become protonated so that they form hydrogen bonding with the ether groups of HEC, resulting in the formation of the micelles. However, we noticed that in the present case of CNipAa copolymer the aggregation starts at a much higher pH value of 4.6, where the complexation between PAA and HEC is not possible.

In fact, there are two pairs of complementary polymers in the present copolymer, i.e., HEC/PAA and PNipAAm/PAA, possible to form interpolymer complexes due to hydrogen bonding as the solution pH decreases. It was reported that PNipAAm shows a stronger complexation interaction with PAA than with HEC, as justified by their critical complexation pH values, i.e., at 4.60 ± 0.02 for the former and 2.80 ± 0.02 for the latter.[22,23] The turning pH point for the aggregation of CNipAa, we observed, is almost the same as the critical pH value of the interpolymer complexation between PAA and PNipAAm. Therefore, we believe that the interpolymer complexation of these two grafts is responsible for the aggregation: as pH decreases to 4.6, PAA and PNipAAm chains form an interpolymer complex, losing their solubility and then forming the insoluble core, while HEC backbones keep soluble and surround the core forming the shell. In short, decreasing pH to 4.6 causes the micellization of CNipAa. In addition, the molar content of AA in the copolymer is only about a half of NipAAm, so after the micellization there are almost no free PAA chain segments left for its further complexation with HEC. The process of pH-induced micellization of graft copolymer CNipAa can be illustrated by the scheme shown in Figure 2.

This mechanism was supported by ^{1}H NMR analysis of CNipAa copolymer in D_2O. As shown in Figure 3, both the characteristic signals of PNiPAAm grafts (at about 1.1, 3.8, and 1.5−2.0 ppm) and PAA grafts (at 1.5−2.0 ppm) undergo weakening at pH 4.6 and almost completely disappear at pH 1.3, while the character signals of HEC do not change over the whole pH range. These results clearly demonstrate that PNiPAAm chains form compact complexes with PAA, while HEC remains solvated.

As pyrene has much lower solubility in water (about 10^{-7} mol/L) than in hydrocarbons (0.075 mol/L), it transfers into hydrophobic domains once such a region forms in aqueous

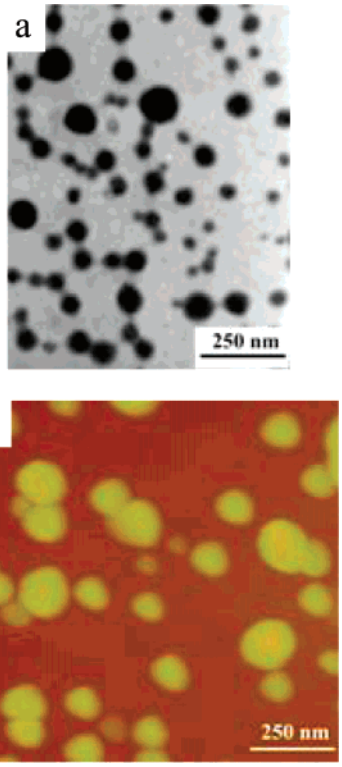

Figure 4. TEM (a) and AFM (b) images for the pH-caused micelles from CNipAa copolymers at pH 1.3 and 30 °C.

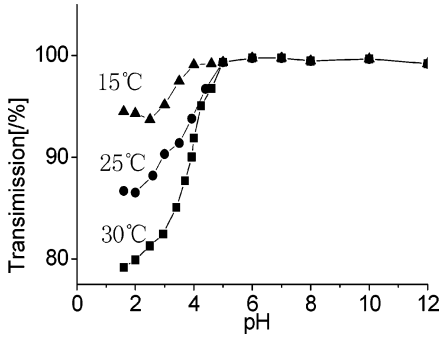

Figure 5. Dependence of turbidity of CNipAa copolymer aqueous solutions on pH at different temperatures.

solution, causing an evident change in the photophysical characters, such as the decrease in the ratio I_1/I_3.[24−27] Therefore, in the present system, pyrene was used to monitor the micellization of CNipAa. With decreasing pH, fluorescence intensity ratios (I_1/I_3) of pyrene experienced an abrupt change from above 1.8 to about 1.5 at the point of 4.6 (Figure S6), which is in good agreement with the critical aggregation pH determined by DLS.

The morphology of the pH-induced micelles was examined by transmission electron microscopy (TEM), atomic force microscopy (AFM), and dynamic/static light scattering (DLS/SLS). As shown in Figure 4a,b, solid spherical aggregates with diameters in the range of 40−130 nm were observed by both TEM and AFM. AFM analysis shows that the heights of the particles are around 20−65 nm, apparently less than but comparable to their diameter, which indicates that these micelles are basically robust and only mildly collapse on the substrate during drying. Moreover, the DLS/SLS measurements also agree with the conclusion of solid spherical structure of these micelles because the micellar $\langle R_g\rangle/\langle R_h\rangle$ ratio is found to be around 0.73 ($\langle R_h\rangle$ 91.58 nm, $\langle R_g\rangle$ 66.4 nm; Figure S11), very close to the theoretic value (0.774) of solid spheres.[14,28] In addition, the

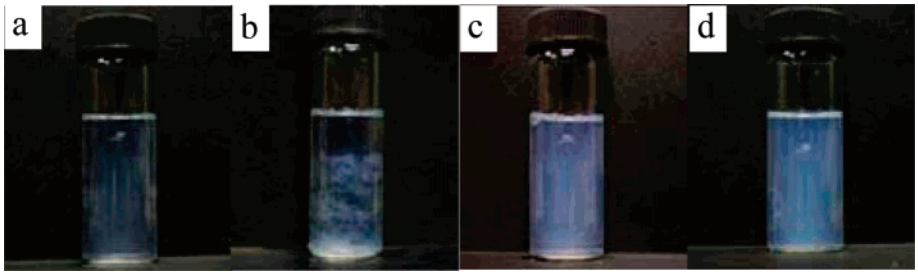

Figure 6. Photos of pH-induced micelles (pH = 1.3) from CNipAa copolymer: (a) prepared and stored at 15 °C; (b) prepared at 15 °C and stored at 45 °C; (c) prepared and stored at 30 °C; (d) prepared at 30 °C and stored at 45 °C.

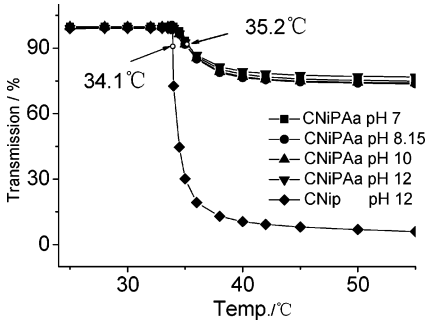

Figure 7. Turbidity changes of CNiPAa and CNip copolymer solutions with increasing temperature at different pH values.

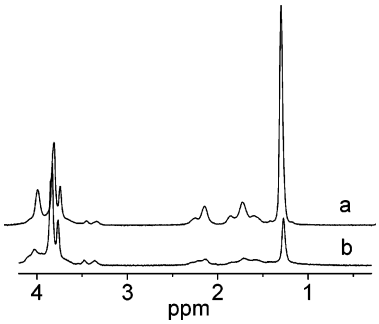

Figure 8. ^{1}H NMR spectra of CNipAa copolymer at pH 12: (a) 25 and (b) 40 °C.

weight-average molar mass M_w and the mass density of these micelles are found to be 1.52×10^7 g/mol (Figure S11, with apparent aggregation number N_{agg}, 42.9) and 7.84×10^{-3} g/mL, respectively. We noticed that the $\langle D_h \rangle$ of the micelles in solution measured by DLS (about 185 nm) is apparently larger than those observed in TEM and AFM since the micelles are swollen in water, while TEM or AFM observations are for the dried particles.

Solution temperature was found to play a significant role in the pH-induced micellization. Staikos et al.[29−31] investigated the effect of temperature on the complexation of homopolymers of PNipAAm and PAA and concluded that PNiPAAm at a higher temperature can form more compact complexes with PAA. Figure 5 shows the light transmission of CNipAa graft copolymer solution as a function of solution pH at 15, 25, and 30 °C. In all the cases, the transmission keeps unvaried over a wide pH range and then suddenly drops down when pH decreases to a certain critical value depending on the solution temperature. As shown in Figure 5, the critical pH value for the complexation is about 4.6, 4.4, and 3.5 for 30, 25, and 15 °C, respectively. As we know, PNiPAAm chains present different hydrophilicity depending on temperature. Even in the temperature range below LCST, increasing temperature still favors the conformation of PNipAAm chains with a higher hydrophobicity although they remain soluble. Such PNiPAAm

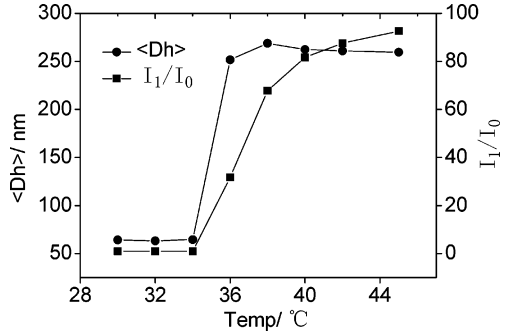

Figure 9. $\langle D_h \rangle$ and I_1/I_0 of CNipAa copolymers as a function of temperature in aqueous solution at pH 12.

chains may result in complexation with PAA occurring at a higher pH value. Similar phenomena were also observed in PNipAAm/PMAA complexation systems by Tenhu.[32]

The temperature at which pH-dependent micellization of CNipAa coplymer took place was also found to influence the stability of the micelles significantly. As shown in Figure 6a,b, the stable micelles prepared at pH 1.3 and 15 °C quickly precipitated in a few minutes when the temperature was elevated to 45 °C. However, the micelles obtained at 30 °C kept stable for dozens of days no matter they were stored at 30 or 45 °C (seen as Figure 6c,d). This difference caused by temperature is understandable. For the case of 15 °C, the PNiPAAm chains are so hydrophilic that they have a weaker inclination to form impact complexes with PAA even in a strong acid medium; thus, many PNipAAm chain segments remain "free" in the resultant micelles. Therefore, when temperature is elevated above LCST, these free segments undergo a thermoinduced phase transition and thus promote the aggregation between micelles. However, for the case of 30 °C, most PNipAAm chains combine with PAA in the micellar core, and there are almost no free PNipAAm chain segments on the surface of the micelles responding to further temperature stimuli; thus, no macroprecipitation takes place for the micelles even when the temperature is elevated to above LCST.

Temperature-Induced Micellization of CNipAa Copolymers. We found that both CNipAa and its precursor copolymer CNip undergo remarkable thermoinduced micellization in water, just as various PNiPAAm-containing block (graft) copolymers do.[33−37] However, differing from those of the PNipAAm-containing copolymers, the thermoinduced micelles of CNipAa have a complex PAA/HEC shell instead of single component one. Interestingly, such a complex shell was found capable of responding to a pH change, leading to a further structural change of the micelles.

As shown by Figure 7, both CNipAa and CNip copolymer solutions turn opaque but not precipitate when the temperature increases to above LCST, which is approximately at 35 °C for CNipAa and 34 °C for CNip. In this process, PNiPAAm grafts

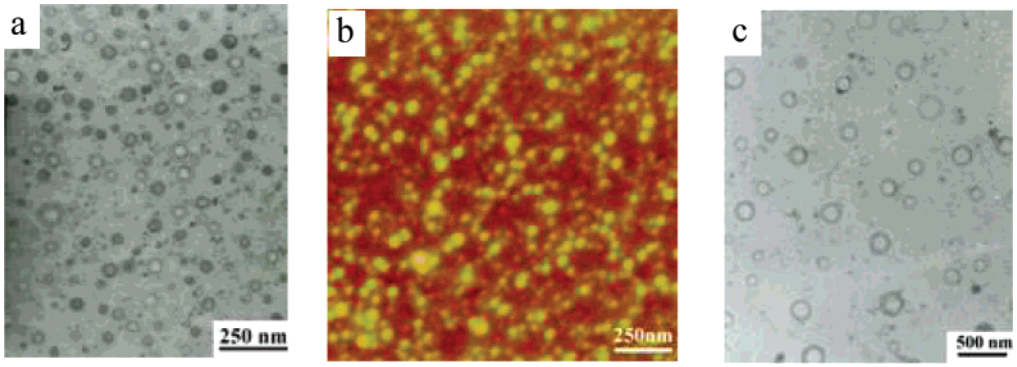

Figure 10. TEM (a) and AFM (b) images for thermoinduced micelles of CNipAa micelles at pH 12 and 45 °C and the TEM image (c) of corresponding micelles of CNip.

Table 2. Characterization Data of Micelles from CNip and CNipAa Copolymers

samples	$\langle R_h \rangle$/nm	polydispersity index (PDI)	$M_w \times 10^{-7}$	$\langle R_g \rangle$	$\langle R_g \rangle / \langle R_h \rangle$	mass density of micelles (10^{-3} g/mL)
thermo-induced micelles of CNip[a]	150.7	0.187	1.44	94.1	0.62	1.67
pH-induced micelles of CNipAa[b]	91.58	0.108	1.52	66.4	0.73	7.84
thermo-induced micelles of CNipAa[c]	124.6	0.116	0.31	87.9	0.71	0.64

[a] Micelles from CNip solution at 45 °C. [b] Micelles from CNipAa solution at pH 1.3 and 30 °C. [c] Micelles from CNipAa solution at pH 12 and 45 °C.

obviously phase-separate from the aqueous solution, leading to micelles with hydrophobic PNiPAAm chains forming the core and the chains of HEC and PAA forming the compound shell. In addition, the solution of CNip copolymer is more turbid than that of the CNipAa as temperature is elevated to above the LCST. Such an apparent discrimination clearly shows the significant role of PAA chains in the micellization of CNipAa; i.e., as PAA grafts are of high hydrophilicity at pH 7−12, they offer a greater hindrance to the aggregation of PNipAAm grafts. As a result, CNipAa forms much smaller micelles than CNip, which was demonstrated by DLS measurements. It is worthy noting that here the LCST of CNipAa copolymer is basically irrespective of pH value of the solution in the measured range of pH 7−12.

This micellization mechanism was confirmed by ^{1}H NMR analysis of CNipAa copolymers in D_2O. Comparing the spectra obtained at 25 and 40 °C (Figure 8), it is obvious that the feature signals of PNiPAAm (at about 1.1, 3.8, and 1.5−2.0 ppm) are largely screened due to the phase transition of PNiPAAm grafts above its LCST. This observation effectively supports the speculation that the core of micelles is formed by PNipAAm grafts rather than others. Besides, pyrene probe measurements also justify this opinion (Figure S7). I_1/I_3 of pyrene sharply decreases from 1.81 to 1.56 with a turning point at ∼35 °C, which is consistent with the cloud point of CNipAa copolymer measured by turbidity. As both PAA chains and HEC backbones are hydrophilic over the measured temperature range, they do not contribute to the core formation. PNipAAm grafts, in this process, are expected to undergo a coil−globule transition above its LCST and form hydrophobic microdomains as the micellar core.It is worthy noting that I_1/I_3(1.56) measured here is higher than that in the conventional micelles of surfactants, signifying that the micellar core composed of PNipAAm grafts possibly is highly hydrated and has a lower mass density.

Figure 9 shows $\langle D_h \rangle$ and the relative scattering intensity I_1/I_0 of CNipAa copolymer solutions at pH 12 with increasing temperature. A dramatic increase of both $\langle D_h \rangle$ and I_1/I_0 took place over a narrow range of 34−36 °C, indicating the formation of the thermoinduced micelles. Afterward, $\langle D_h \rangle$ keeps constant at about 250 nm but I_1/I_0 continuously augments, indicating that the micelles become more compact with temperature increase.

The shape and size of the thermoinduced micelles were studied via TEM and AFM observations. As shown by Figure 10a,b, these micelles are of spherical shape with diameters ranging from 30 to 65 nm. AFM height analysis shows that the heights of the micelles are in the range of 10−20 nm, nearly one-third of the diameter of micelles, implying moderate collapse of the micelles on mica substrate. However, to our surprise, in the TEM images of the thermoinduced micelles at appearance have central cavities. This "hollow structure" obviously conflicts with the assumptive core−shell structure of the micelles. Hence, a combination of DLS/SLS was used to measure the $\langle R_g \rangle / \langle R_h \rangle$ ratio of the micelles, which was useful to clarify the discrepancy. The $\langle R_g \rangle / \langle R_h \rangle$ was found to be about 0.71 ($\langle R_g \rangle$ 87.9 nm, Table 2 and Figure S11), very close to the theoretic value 0.774 of the standard solid sphere. So we tend to think of the micelles in solution as solid spheres.[14,28] The apparent cavitary images in TEM, in our opinion, were probably caused during drying of the micelles: the surface of the micelle dried quicker than the interior owing to uneven evaporation of water, and then the polymer chains in the core were likely to shrink toward the predried surface causing the cavity. If this argument is correct, similar cavitary structure is expected for the thermoinduced micelles of copolymer CNip having PNipAAm grafts alone. As seen in Figure 10c, we indeed observed hollow spherical morphology. Meanwhile, these micelles in solution have a $\langle R_g \rangle / \langle R_h \rangle$ 0.62 (Table 2 and Figure S11), implying solid spherical particles too. It is worthy noting that the size about 250 nm of the micelles from CNipAa measured by DLS is 4−5 times larger than that observed by TEM, which indicates a huge deswelling during the drying process of the micellar samples. This is probably attributed to the fact that part of the hydrophilic chains (such as HEC) covalently bonded to PNiPAAm grafts were likely wrapped into the core leading to a highly hydrated core with a lower mass density. This speculation was supported by an additional DLS/SLS measurement; i.e., the mass density of the thermoinduced CNipAa micelles (0.64×10^{-3} g/mL) is much lower than that of pH-caused micelles (7.84×10^{-3} g/mL). The related measurement results of various micelles from CNipAa and its precursor CNip via DLS/SLS are summarized in Table 2.

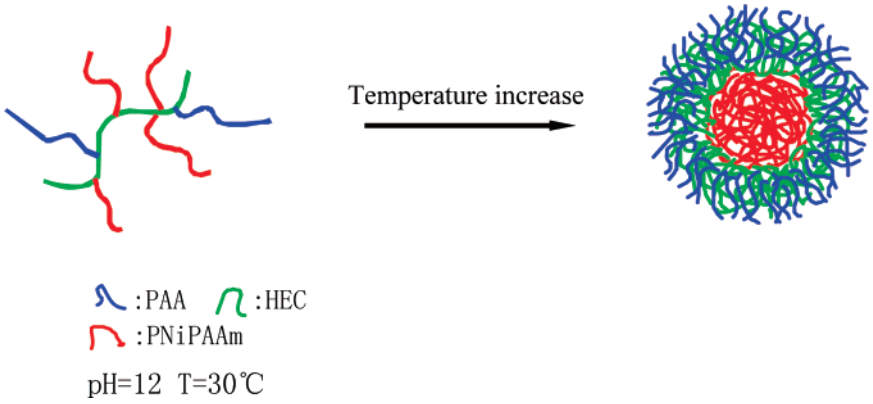

Figure 11. A proposed scheme of the formation of temperature-induced micellization from CNipAa-1 copolymer at pH 12.

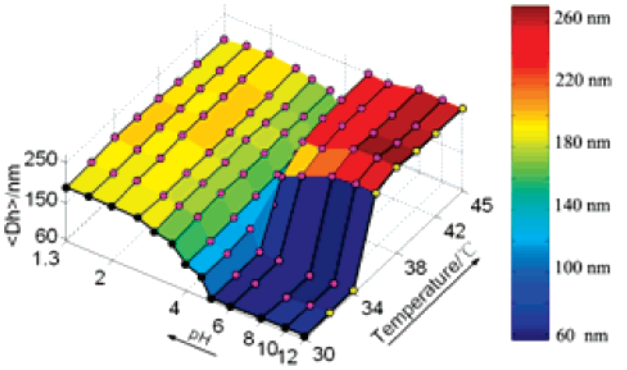

Figure 12. Three-dimensional profile of the dependences of $\langle D_h \rangle$ of CNipAa on temperature over the wide pH range from 1.3 to 12. First, a series of CNipAa solutions with given pH values were prepared at 30 °C, followed by increasing temperature from 30 to 45 °C. $\langle D_h \rangle$ was measured after the micelles were kept for 1 h at the desired temperature.

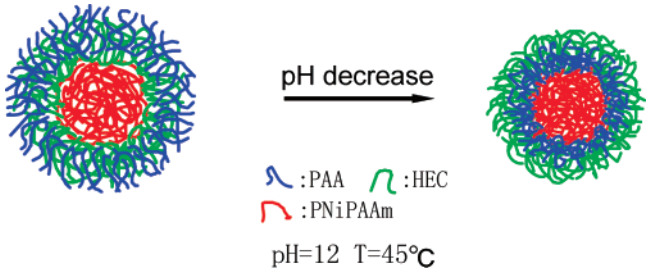

Figure 13. A proposed scheme of the acidification process of thermoinduced micelles from CNipAa copolymer at pH 12 and 45 °C.

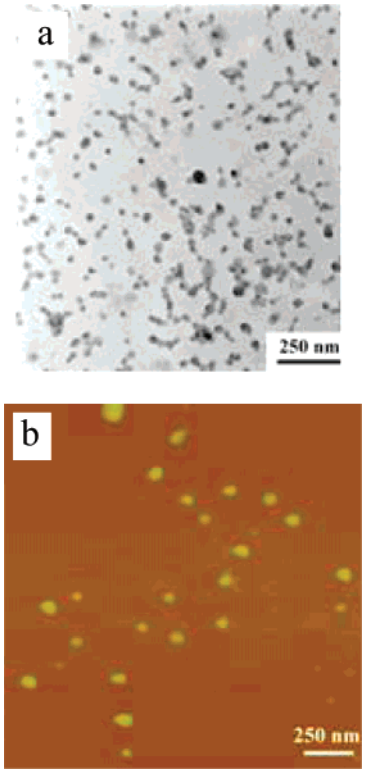

Figure 14. TEM (a) and AFM (b) images of acidified thermoinduced micelles of CNipAa copolymers at pH 1.3 and 45 °C.

Based on all the results discussed above, the thermoinduced micellization of CNipAa copolymer can be illustrated by the scheme shown in Figure 11.

Further Response of pH-Induced and Temperature-Induced Micelles. As shown in Figure 12, a three-dimension profile was drawn to give an overview of the dependences of $\langle D_h \rangle$ of CNipAa copolymer solutions on temperature over the whole pH range. For constructing this figure, $\langle D_h \rangle$ was first measured for a series of CNipAa copolymer solutions with given pH values prepared at 30 °C, and then these solutions were monitored to acquire their $\langle D_h \rangle$ variations with increasing temperature from 30 to 45 °C. The black points in the brim of Figure 12 shows the pH-induced micellization of CNipAa at 30 °C, while the yellow points refer to the thermoinduced micellization at pH 12; both have been discussed in details above. Figure 12 also shows that the solutions in the pH range of 4.6−12 display similar thermal sensitivity and undergo abrupt leaps in $\langle D_h \rangle$ over a narrow range of 34−36 °C, irrespective of solution pH. From the figure, we observe clearly the effect of the thermal stimulus on the pH-induced micelles. The pH-induced micelles show different response to increasing temperature from 30 to 45 °C depending on pH. For the micelles formed at pH 3.0−4.6, a substantial increase in $\langle D_h \rangle$ from about 120 to 160 nm was found with increasing temperature, while $\langle D_h \rangle$ remained unvaried upon pH < 3.0. Typical examples of the two cases (pH 1.3 and 1.6) can be seen in Figure S8. In our opinion, the complexation of PAA and PNipAAm is insufficient at pH 4.6 so that a part of PNipAAm chain segments keep "free" in solution, which may further respond to increasing temperature and cause an increase of $\langle D_h \rangle$. However, for the solutions below pH 3.0, most PNipAAm chain segments are involved in forming compact complexes with PAA and stay inside the micelles. Hence, subsequent increasing temperature hardly influences the diameter of micelles.

It should be noted that the further responding behavior of the thermoinduced micelles of CNipAa to pH is not shown in Figure 12. As mentioned above, the thermoinduced micelles in basic solution have compound shell of HEC/PAA chains. When the pH of the micellar solution decreases to 1.3 directly, a

remarkable $\langle D_h \rangle$ decrease from 260 to 190 nm was observed by DLS. Obviously, this pH decrease would cause protonation of the PAA chains in the shell, leading to forming complex with the PNipAAm chains and collapse. As a result, a new inner shell mainly composed of the complexes of PAA and PNiPAAm is generated. Thus, these acidified thermoinduced micelles are expected to have a three-layer structure; i.e., the hydrophobic PNiPAAm chains form the core and the insoluble complexes of PAA/ PNiPAAM chains form the inner shell, and solvated HEC chains form the outer shell (Figure 13). Surprisingly, the diameters of these micelles keep unvaried even when temperature returns from 45 to 30 °C, below the LCST. It implies that in these acidified thermoinduced micelles the PNipAAm chains, to some extent, are "locked" by hydrogen-bonding complexation with PAA chains. Thus, PNipAAm chains are no longer able to perform their globule−coil transition when temperature decreases to below the LCST.

The morphology of the acidified thermoinduced micelles was studied by TEM and AFM. As shown by TEM image in Figure 14a, the diameters of the solid spherical particles are in the range of 30−55 nm, in good agreement with that observed by AFM (Figure 14b). Meanwhile, the height analysis indicates that the micellar heights are in the range of 15−25 nm.

Conclusions

CNipAa copolymers are capable of self-assembling into three forms of nanosize micellar structures driven by external pH and temperature changes. In the process, hydrogen-bonding interaction of the complementary grafts, PNiPAAm and PAA, and hydrophobic aggregation of PNiPAAm play a crucial role. Because of pH changes, the micelles with PNipAAm/PAA complex as the core and solvated HEC as the shell can be obtained below pH 4.6. The CNipAa copolymer in solution with pH > 4.6 can self-assemble into micelles with PNipAAm grafts as the core and HEC/PAA as the compound shell when the temperature is elevated above the LSCT of PNipAAm. These thermoinduced micelles can further respond to pH change, resulting in the formation of the micelles with a three-layer structure. All the three forms of micellar structure were investigated by TEM and AFM as well as DLS/SLS.

Acknowledgment. We acknowledge the financial support from the National Science Foundation of China (No. 50333010).

Supporting Information Available: Text giving the details of synthesis and characteristics of binary graft copolymer CNipAa and its precursor CNip. This material is available free of charge via the Internet at http://pubs.acs.org.

References and Notes

(1) Butun, V.; Billingham, N. C.; Armes, S. P. *J. Am. Chem. Soc.* **1998**, *120*, 11818−11819.
(2) Butun, V.; Billingham, N. C.; Armes, S. P.; et al. *Macromolecules* **2001**, *34*, 1503−1511.
(3) Liu, S. Y.; Billingham, N. C.; Armes, S. P. *Angew. Chem., Int. Ed.* **2001**, *40*, 2328−2331.
(4) Liu, S. Y.; Armes, S. P. *Angew. Chem., Int. Ed.* **2002**, *41*, 1413−1417.
(5) Liu, S. Y.; Armes, S. P. *Langmuir* **2003**, *19*, 4432−4438.
(6) Gohy, J. F.; Creutz, S.; Garcia, M.; Mahltig, B.; Stamm, M.; Jerome, R. *Macromolecules* **2000**, *33*, 6378.
(7) Dai, S.; Ravi, P.; Tam, K. C.; Mao, B. W.; Gan, L. H. *Langmuir* **2003**, *19*, 5175.
(8) Bories-Azeau, X.; Armes, S. P.; Van den Haak, H. J. W. *Macromolecules* **2004**, *37*, 2348.
(9) Schilli, C. M.; Zhang, M. F.; Rizzardo, E.; et al. *Macromolecules* **2004**, *37*, 7861−7866.
(10) Andre, X.; Zhang, M. F.; Muller, A. H. E. *Macromol. Rapid Commun.* **2005**, *26*, 558−563.
(11) Zhang, W. Q.; Shi, L. Q.; Ma, R. J. *Macromolecules* **2005**, *38*, 8850−8852.
(12) Butun, V.; Top, R. B.; Ufuklar, S. *Macromolecules* **2006**, *39*, 1216−1225.
(13) Cai, Y. L.; Armes, S. P. *Macromolecules* **2004**, *37*, 7116−7122.
(14) Dou, H. J.; Jiang, M. *Angew. Chem., Int. Ed.* **2003**, *42*, 1516−1519.
(15) Butun, V.; Billingham, N. C.; Armes, S. P. *Macromolecules* **2000**, *33*, 6378−6387.
(16) Butun, V.; Billingham, N. C.; Armes, S. P. *Polymer* **2000**, *41*, 3173−3182.
(17) Butun, V.; Wang, X. S.; Banez, M. V. *Macromolecules* **2000**, *33*, 1−3.
(18) Weaver, J. M.; Arotcarena, M.; Heise, B.; Ishaya, S.; Laschewsky, A.; Tenhu, H. *Langmuir* **2002**, *124*, 3787.
(19) Butun, V.; Billingham, N. C.; Armes, S. P. *J. Am. Chem. Soc.* **1998**, *120*, 12135.
(20) Yao, X. M.; Chen, D. Y.; Jiang, M. *J. Phys. Chem. B* **2004**, *108*, 5225−5229.
(21) Zhang, G.; Wu, C. *J. Am. Chem. Soc.* **2000**, *122*, 10201.
(22) Khutoryanskiy, V. V.; Mun, G. A.; Nurkeeva, Z. S. *Polym. Int.* **2004**, *53*, 1382−1387.
(23) Nurkeeva, Z.; Mun, G. A.; Khutoryanskiy, V. V. *Macromol. Biosci.* **2003**, *3*, 283−295.
(24) Chu, D. Y.; Thomas, J. K. *Macromolecules* **1987**, *20*, 2133−2138.
(25) Kalyanasundaram, K.; Thomas, J. K. *J. Am. Chem. Soc.* **1977**, *99*, 2039−2044.
(26) Li, M.; Jiang, M.; Wu, C. *J. Polym. Sci., Part B: Polym. Phys.* **1997**, *35*, 1593−1599.
(27) Kagej, K.; Skerjanc, J. *Langmuir* **1999**, *15*, 4251−4258.
(28) Wu, C.; Zhou, S. Q. *Phys. Rev. Lett.* **1996**, *77*, 3053.
(29) Staikos, G.; Bokias, G.; Karayanni, K. *Polym. Int.* **1996**, *41*, 345−350.
(30) Staikos, G.; Karayanni, K.; Mylonas, Y. *Macromol. Chem. Phys.* **1997**, *198*, 2905−2915.
(31) Jones, M. S. *Eur. Polym. J.* **1999**, *35*, 795−801.
(32) Burova, T. V.; Natalia, V.; Grinberg, V. Y. *Macromolecules* **2005**, *38*, 1292−1299.
(33) Schild, H. G. *Prog. Polym. Sci.* **1992**, *17*, 163−249.
(34) Chen, G. H.; Hoffman, A. S. *Nature (London)* **1995**, *373*, 49−51.
(35) Topp, M. D. C.; Dijkstra, P. J.; Talsma, H.; Feijen, J. *Macromolecules* **1997**, *30*, 8518−8520.
(36) Hsu, Y. H.; Chiang, W. H.; Chen, C. H.; et al. *Macromolecules* **2005**, *38*, 9757−9765.
(37) Gil, E. S.; Hudson, S. M. *Prog. Polym. Sci.* **2004**, *29*, 1173−1222.

MA070147B